33rd Annual International Conference of the IEEE EMBS
Boston, Massachusetts USA, August 30 - September 3, 2011

Blind Separation and Localization of Correlated P300 Subcomponents from Single Trial Recordings Using Extended PARAFAC2 Tensor Model

Bahador Makkiabadi, Delaram Jarchi, and Saeid Sanei
NICE Group, Faculty of Engineering and Physical Sciences, University of Surrey, Guildford, UK

Abstract— **A novel mathematical model based on multi-way data construction and analysis with the goal of simultaneously separating and localizing the brain sources specially the sub-components of event related potentials (ERPs) is introduced. We represent multi-channel EEG data using a third-order tensor with modes: space (channels), time samples, and number of segments. Then, a multi-way technique, in particular, generalized version of PARAFAC2 method, is developed to blindly separate and localize mutually/temporally correlated P3a and P3b sources as subcomponents of P300 signal. In this paper the non-orthogonality of the ERP subcomponents is defined within the tensor model. In order to obtain essentially unique estimation of the signal components one parametric and one structural constraint are defined and imposed. The method is applied to both simulated and real data and has been shown to perform very well even in low signal to noise ratio situations. In addition, the method is compared with spatial principal component analysis (sPCA) and its superiority is demonstrated by using simulated signals.**

I. Introduction

Event related potentials (ERPs) occur as the response of the brain to any audio, visual, or somatosensory stimulus. P300 is a positive ERP which occurs with a latency of about 300 ms after rare or task relevant stimuli and may be further decomposed into the temporally and mutually correlated P3a and P3b subcomponents that overlap over the scalp. P3b is mainly distributed over the centroparietal region and is mostly generated by posterior temporal, parietal, and posterior cingulate mechanisms. P3b has a more centroparietal distribution and corresponds to the classical P300 recorded within an oddball paradigm after rare and task relevant events. P3a occurs after novel events independently of task relevance and is characterized by a more frontal distribution, a shorter latency, and fast habituation. P300 and its subcomponents have significant diagnostic and prognostic potential especially when its evaluation is combined with other clinical assessment methods [1]. So, it is necessary to develop efficient and robust methods for separation and localization of P300 and also its subcomponents. Blind source separation (BSS) has been proposed for this purpose by a number researchers such as in [2]. There are some well established principle component analysis (PCA) based methods aiming at separation of the correlated sources. These methods are divided into two categories, temporal-PCA which is designed for estimation of temporally uncorrelated signals and spatial-PCA for spatially uncorrelated signals such as in [3]. On the other hand, tensor factorization has been used to tackle the BSS of brain sources for the past two decades [4]. Recently, a tensor factorization based method is developed to separate the brain sources in time domain [5]. This method employs parallel factor analysis (PARAFAC) extension called PARAFAC2 [6] tensor model for the temporally segmented mixture signals. Later, a similar concept has been used to separate the brain sources in time-frequency domain [7]. This paper is an improved version of previous work in [5] for separating correlated P3a and P3b. The remainder of the paper is structured as follows. In Section II our model and its problem formulation is described. In Section III estimation of model parameters is provided. In Section IV the results of applying the method to simulated and real data are provided. Finally Section V concludes the paper.

II. Model and Problem Formulation

Consider the following instantaneous mixing system:

$$\mathbf{X} = \mathbf{S}\mathbf{A}^T + \mathbf{V} \tag{1}$$

where $\mathbf{X} \in \mathbb{R}^{N \times N_x}$, $\mathbf{S} \in \mathbb{R}^{N \times N_s}$, and $\mathbf{V} \in \mathbb{R}^{N \times N_x}$ denote respectively the matrices of observed signals, source signals, and noise. $\mathbf{A} \in \mathbb{R}^{N_x \times N_s}$ is the mixing matrix and N_s and N_x are respectively the number of sources and sensors. Recovering the sources from the acquired mixtures has been investigated by incorporating different assumptions about the sources or mixing systems. Here, it is assumed that the system is overdetermined, i.e., $N_x \geq N_s$. In recent years a number of solutions to BSS problem have been proposed. In these approaches some properties of the sources such as, statistical independence, uncorrelatedness, disjointedness, sparsity, or non-Gaussianity are taken into account. These methods fail when the sources are mutually overlapped or correlated. So, a new method must be developed to solve the blind separation of overlapped sources (BSOS). Tensor factorization is a powerful method which has been used for blind source separation of orthogonal source signals [5]. The main contribution of this paper is therefore incorporating correlatedness of the sources into the tensor model. Similar to the method proposed in [5], in this work a simple temporal segmentation procedure has been used to produce the data tensor by dividing the signals $\mathbf{X}$ and consequently $\mathbf{S}$ to K segments called respectively as $\mathbf{X}_k$ and $\mathbf{S}_k$ with/without overlap and with segment size of N_K. Having overlapped $\mathbf{S}_k$s is an important criterion which must be considered. So, considering correlatedness of the sources for each segment, the original PARAFAC2 model is changed to:

$$\begin{aligned} &\mathbf{X}_k = \mathbf{S}_k\mathbf{A}^T + \mathbf{V}_k \\ &\mathbf{S}_k^T\mathbf{S}_k = \mathbf{R}_k\mathbf{D}_k^2; \forall\ k = 1, \ldots, K \end{aligned} \tag{2}$$

where $\mathbf{X}_k \in \mathbb{R}^{N_k \times N_x}$ and $\mathbf{S}_k \in \mathbb{R}^{N_k \times N_s}$ are mixture and source signals, $\mathbf{R}_k$ is the correlation matrix, and finally $\mathbf{D}_k^2$ is a positive diagonal matrix which shows the power of each source signal for each segment k. Note that, for orthogonal or independent sources $\mathbf{R}_k$ is very close to identity matrix. For simplicity, we ignore the noise term $\mathbf{V}_k$. Also, based on above formulation, we can factorize each $\mathbf{S}_k$ into an orthonormal matrix $\mathbf{P}_k$, a similarity matrix $\mathbf{H}_k$, and a diagonal matrix $\mathbf{D}_k$, which absorbs the norm of different sources at each segment k. So, based on the above decomposition, the model in (2) can be rewritten as:

$$\begin{aligned} &\mathbf{X}_k = \mathbf{P}_k\mathbf{H}_k\mathbf{D}_k\mathbf{A}^T \\ &\mathbf{P}_k^T\mathbf{P}_k = \mathbf{I}_{N_s}; \mathbf{R}_k = \mathbf{H}_k^T\mathbf{H}_k; \forall\ k = 1, \ldots, K \end{aligned} \tag{3}$$

where $\mathbf{I}_{N_s} \in \mathbb{R}^{N_s \times N_s}$ is an identity matrix. Actually the above formulation tries to model the data tensor which includes all $\mathbf{X}_k$s. The proposed model can be considered as generalization of the traditional PARAFAC2 tensor model for each $\mathbf{X}_k$ as $\mathbf{X}_k = \mathbf{P}_k\mathbf{H}\mathbf{D}_k\mathbf{A}^T$, where $\mathbf{H}$ is a fixed matrix for all segments. Recently, PARAFAC2 has been used to separate the normal brain rhythms in time domain [5] and time-frequency domains [7]. Compared to the PARAFAC2 model, having different $\mathbf{H}_k$s rather than a fixed $\mathbf{H}$ for all ks gives more flexibility to the proposed model. It is concluded that this model may not provide unique decomposition of every segmented mixture $\mathbf{X}_k$. However, by considering different constraints for the parameter of this model, i.e., all $\mathbf{P}_k$s are supposed to be orthonormal, all $\mathbf{D}_k$s are supposed to be diagonal matrices, and all $\mathbf{R}_k$ are supposed to be correlation matrices, it practically leads to unique estimations. Moreover, in some applications other constraints such as orthogonality (orthogonality of columns of $\mathbf{A}$) or non-negativity can be considered for the mixing system. Having unique estimations for the parameters of the proposed model solves the localization problem by estimating $\mathbf{A}$. It also solves the BSOS problem using the information about all $\mathbf{D}_k$s, $\mathbf{H}_k$s, and $\mathbf{P}_k$s to reconstruct the segmented sources as $\mathbf{S}_k$. The next section introduces the process for estimating all the parameters of the above tensor model.

III. Estimation of the Model Parameters

Recalling the main formulation for each segment $\mathbf{X}_k = \mathbf{P}_k\mathbf{D}_k\mathbf{A}^T$ the overall minimization problem can be defined as:

978-1-4244-4122-8/11/$26.00 ©2011 IEEE

$$J = \sum_{k=1}^{K} ||\mathbf{X}_k - \mathbf{P}_k\mathbf{H}_k\mathbf{D}_k\mathbf{A}^T||_F^2 \quad (4)$$

where $||.||_F$ stands for Frobenius norm of a matrix. In order to fit the model of mixtures, alternating least squares (ALS) minimization is developed for estimation of the two set of parameters separately. The following procedures are used to estimate $\mathbf{P}_k$s, $\mathbf{A}$, $\mathbf{H}_k$s, and $\mathbf{D}_k$s.

Estimation of $\mathbf{P}_k$: Let's assume that $\mathbf{A}$, $\mathbf{H}_k$s, and $\mathbf{D}_k$s are known for all k and estimation of all orthonormal $\mathbf{P}_k$s is required. The cost function for each k can be introduced as:

$$\begin{aligned} J_{P_k} =& tr(\mathbf{X}_k^T\mathbf{X}_k)+ \\ & tr(\mathbf{A}(\mathbf{D}_k\mathbf{R}_k\mathbf{D}_k)\mathbf{A}^T) - tr(2\mathbf{A}\mathbf{D}_k\mathbf{H}_k^T\mathbf{P}_k^T\mathbf{X}_k) \end{aligned} \quad (5)$$

which has to be minimized. Obviously, the first two terms of the above cost function are independent of $\mathbf{P}_k$ and positive semi-definite (PSD) matrices (their trace values are nonnegative). So, the above minimization problem can be converted to maximization of $tr(\mathbf{P}_k\mathbf{H}_k\mathbf{D}_k\mathbf{A}^T\mathbf{X}_k^T)$. In order to achieve this, we define a new variable $\mathbf{Z}_k$ and its singular value decomposition (SVD) as:

$$\mathbf{Z}_k = \mathbf{H}_k\mathbf{D}_k\mathbf{A}^T\mathbf{X}_k^T = \mathbf{U}_k\mathbf{\Sigma}_k\mathbf{V}_k^T \quad (6)$$

where $\mathbf{\Sigma}_k$ is a diagonal matrix with nonnegative diagonal elements and two orthonormal $\mathbf{U}_k$ and $\mathbf{V}_k$ matrices. Then, it can be proved that one of the best estimations of $\mathbf{P}_k$ can be obtained as:

$$\mathbf{P}_k = \mathbf{V}_k\mathbf{U}_k^T \quad (7)$$

Estimation of $\mathbf{A}$***,*** $\mathbf{H}_k$***s, and*** $\mathbf{D}_k$***s***: Generally, each one of $\mathbf{A}$, $\mathbf{H}_k$s, and $\mathbf{D}_k$s can be estimated as a part of the ALS optimization (estimate one of them when all other parameters are considered fixed). However, in this paper a closed form solution for estimation of all above parameters using Tucker based tensor factorization is presented. Assume that all $\mathbf{P}_k$ matrices are estimated and let's define a new tensor which includes $\mathbf{Y}_k$ slabs as:

$$\mathbf{Y}_k = \mathbf{X}_k^T\mathbf{P}_k \quad (8)$$

Having orthogonal $\mathbf{P}_k$ and using the main model of $\mathbf{X}_k$ defined in (3) implies

$$\mathbf{Y}_k = \mathbf{A}\mathbf{G}_k \quad (9)$$

where $\mathbf{G}_k = \mathbf{D}_k\mathbf{H}_k^T$. The tensor $Y \in R^{N_x \times N_s \times K}$ includes $\mathbf{Y}_k$s and subsequently $\mathbf{G}_k$s. $G \in R^{N_s \times N_s \times K}$ is called core tensor. If all $\mathbf{H}_k$ were the same and equal to a fixed $\mathbf{H}$ the best tensor model for Y would be a simple PARAFAC model. Also, if $\mathbf{H}_k$s were assumed orthogonal PARAFAC2 could be the best model for factorization of tensor Y with $\mathbf{Y}_k$ slabs. However, in current application with overlapped sources non of the above assumptions are valid and therefore Tucker tensor model is preferred. This model supports non-diagonal core tensor slabs (in contrary to Kruskal structure of PARAFAC model in which the core tensor slabs are diagonal) [8]. Here the Tucker tensor model is briefly explained first. Then, it is employed to estimate $\mathbf{A}$, $\mathbf{H}_k$s, and $\mathbf{D}_k$s.

1) Tucker model: Tucker model is generalization of SVD decomposition for tensors. Analogous to SVD/PCA for modeling each matrix $\mathbf{X} \in R^{I \times J}$ comprising of F components we have $x_{ij} \approx \sum_{f=1}^{F} a_{if}b_{jf}g_{ff}$, where g_{ff} are proportional to the eigenvalues. Similar to SVD decomposition for our application, Tucker3 [9] can model a tensor $X \in R^{I \times J \times K}$ with N_s factors in all its three modes (in general case number of factors for different modes can be different but here they are considered equal) as $x_{ijk} \approx \sum_{d=1}^{N_s}\sum_{e=1}^{N_s}\sum_{f=1}^{N_s} a_{id}b_{je}c_{kf}g_{def}$. As it can be seen there is a core tensor G with g_{def} elements which is one part of the Tucker3 model. Also there are simplified extensions of Tucker3 model which have less parameters, such as Tucker2 in which $x_{ijk} \approx \sum_{d=1}^{N_s}\sum_{e=1}^{N_s} a_{id}b_{je}g_{dek}$, and Tucker1 represented by $x_{ijk} \approx \sum_{d=1}^{N_s} a_{id}g_{djk}$. Generally, unlike PARAFAC based models, the Tucker tensor factorization approach does not have unique results. However, by imposing some restrictions on the model, it tends to converge to a unique solution [8]. Here, Tucker1 has been chosen to model the tensor Y to estimate the mixing channel $\mathbf{A}$ as the factor related to the first mode and $\mathbf{H}_k$s and $\mathbf{D}_k$s as the decomposition of core tensor matrices simultaneously. Based on our assumptions $\mathbf{R}_k = \mathbf{H}_k^T\mathbf{H}_k$s are supposed to be the correlation matrices. This imposes a constraint to the core tensor to create a specific structure with symmetric or specifically PSD matrices at each slab along k. Moreover, non-negativity constraint on mixing gains $\mathbf{A}$ is considered to obtain unique estimation of the parameters.

In order to estimate the parameters equation (9) can be rewritten as:

$$\mathbf{Y} = \mathbf{A}\mathbf{G} \quad (10)$$

where $\mathbf{Y} \in R^{N_x \times (N_s \times K)}$ and $\mathbf{G} \in R^{N_s \times (N_s \times K)}$ are respectively unfolded versions of Y and G.

2) Estimation of A: In an unconstrained scenario $\mathbf{A}$ can be estimated easily as:

$$\mathbf{A} = \mathbf{Y}\mathbf{G}^{\dagger} \quad (11)$$

where $(.)^{\dagger}$ denotes pseudo-inverse operator. However, in the case of having non-negative constraint on $\mathbf{A}$, a minimization problem can be defined to minimize the cost function J_n as:

$$\begin{aligned} & J_n = ||\mathbf{Y} - \mathbf{A}\mathbf{G}||_F \\ & s.t.\ \ a_{ij} \geq 0 \end{aligned} \quad (12)$$

where a_{ij}s are the elements of matrix $\mathbf{A}$. Above optimization problem can be divided into some sub-problems for estimating each row of $\mathbf{A}$ separately as:

$$\begin{aligned} & J_{ni} = ||\mathbf{y}_i^T - \mathbf{G}^T\mathbf{a}_i^T|| \\ & s.t.\ \ a_i \geq 0\ \ for\ \ i = 1, ..., N_x \end{aligned} \quad (13)$$

where $\mathbf{y}_i$ and $\mathbf{a}_i$ denote respectively the ith row of $\mathbf{Y}$ and $\mathbf{A}$. There are some standard solutions for the above sub-problem such as non-negative least squares (NNLS) or fast-NNLS [8],[10].

3) Estimation of $\mathbf{H}_k s$ and $\mathbf{D}_k s$: To estimate $\mathbf{H}_k$s and $\mathbf{D}_k$s it is necessary to estimate the core tensor G by estimation of its unfolded version $\mathbf{G}$. In an unconstrained scenario, estimation of $\mathbf{G}$ can be simply performed by:

$$\mathbf{G} = \mathbf{A}^{\dagger}\mathbf{Y} \quad (14)$$

However, in case of having structural constraint it is necessary to have symmetric PSD $\mathbf{R}_k$s matrices. As our constraint is not defined for $\mathbf{H}_k$s directly a new variable $\mathbf{Q}_k$ is defined to deal with covariance matrix of each $\mathbf{G}_k$ as:

$$\mathbf{Q}_k = Sqrt(\mathbf{G}_k^T\mathbf{G}_k) \quad (15)$$

where $Sqrt(.)$ denotes square root of a square matrix. This operator is different from the operator which takes square root of all elements of matrix separately; for more information refer to [11]. Above procedure tries to obtain $\mathbf{Q}_k$ as the nearest (or one of the nearest) PSD matrices to $\mathbf{G}_k$. After obtaining the PSD $\mathbf{Q}_k$, the target parameters $\mathbf{H}_k$ and $\mathbf{D}_k$ can be easily estimated by:

$$\begin{aligned} & \mathbf{H}_k = \mathbf{Q}_k diag(\mathbf{v}_k)^{\dagger} \\ & \mathbf{D}_k = diag(\mathbf{v}_k) \end{aligned} \quad (16)$$

where $\mathbf{v}_k$ is a vector which contains the column vector norm of $\mathbf{Q}_k$ and $diag(.)$ builds a diagonal matrix with diagonal elements equal to elements of the input vector. It can be seen that the columns of $\mathbf{H}_k$ are normalized and also its covariance $\mathbf{R}_k = \mathbf{H}_k^T\mathbf{H}_k$ builds a correlation matrix. Moreover, the diagonal values of $\mathbf{D}_k$ show the norm of each source vector in segment k.

The final ALS algorithm for estimation of all the parameters of BSOS system is shown in Algorithm 1.

Algorithm 1 ALS Parameter Estimation of BSOS

Step 1 : Initialize all the model parameters randomly.
Step 2 : Estimate $\mathbf{P}_k$ using (7) for all $k = 1, ..., K$.
Step 3 : Solve (13) and estimate all rows of $\mathbf{A}$ using $\mathbf{a}_i^T = NNLS(\mathbf{G}^T, \mathbf{y}_i^T)$ for $i = 1, ..., N_x$.
Step 4 : Calculating $\mathbf{G}$ using (14), (15) and computing all $\mathbf{H}_k$s and $\mathbf{D}_k s$ for $k = 1, ..., K$.
Step 5 : Check the convergence rate $\sigma = ||J_{new} - J_{old}||/||J_{old}||$ if $\sigma > \epsilon$, go to **Step 2** till convergence

4) Using BSOS for ERP subcomponent detection: By exploiting non-negativity of mixing gains to $\mathbf{A}$, super symmetrical structure of the core tensor built by $\mathbf{G}_k$s, and orthogonality of all $\mathbf{P}_k$s, a unique solution is expected. However, in ERP source separation application having non-negative $\mathbf{A}$ may not be valid. The proposed Tucker based model using unconstrained $\mathbf{A}$ may not have unique estimation of the sources, for example, in this case a separated source may be a mixture of P3a and P3b signals and the second one is noise. Typically, the brain sources are considered as dipoles in a forward model of the brain and based on the directions of dipoles the mixing channels can be divided into those with positive and negative gains depending on their position in the brain. So, a group of mixing gains which are related to spatially neighboring electrodes have the same polarity. This fact can be used to provide sub-optimum initial values for the unconstrained algorithm (with no constraint on $\mathbf{A}$) using the results of constrained (with non-negativity constraint on $\mathbf{A}$) algorithm. Therefore, if Algorithm 1, which considers the mixing gains as positive, is applied to the mixture of P3a and P3b signals for few iterations, the algorithm will try to estimate a group of mixing gains that have the same polarity and consider them as non-negative channel information. All other mixing gains are considered to be zero. Since, not all the gains are necessarily positive, this solution is not considered as a general solution but it can be considered as a suitable initial value for an unconstrained algorithm which does not impose any constraint on the estimated $\mathbf{A}$.

The final procedure for separating ERP subcomponent is shown in Algorithm 2. In the next section the latter algorithm is applied

Algorithm 2 Estimation of BSOS parameters for separation of ERP subcomponents

Step 1 : Produce the tensor model of mixture signals using temporal segmentation.
Step 2 : Apply algorithm 1 for the produced tensor few iterations (by choosing large σ such as $\sigma = 0.1$).
Step 3 : Estimation of $\mathbf{P}_k$ using (7) for all $k = 1, ..., K$.
Step 4 : Estimate unconstrained $\mathbf{A}$ using (11).
Step 5 : Calculating $\mathbf{G}$ using (14), (15) and computing all $\mathbf{H}_k$s and $\mathbf{D}_k s$ for $k = 1, ..., K$.
Step 6 : Check the convergence rate $\sigma = ||J_{new} - J_{old}||/||J_{old}||$ if $\sigma > \epsilon$, go to **Step 2** till convergence

to both simulated and real signals and the performance is shown by comparing the results with those of standard spatial PCA method.

IV. Experimental Results

Several simulations were carried out to validate and demonstrate application of the proposed method. Moreover, the method is applied to real EEG recordings for normal subject to separate P300 subcomponents blindly. For real data study, the method was applied to 30 different trials (related to target stimuli) for one subject. All simulated and experimental data were compared with spatial-PCA separation method using ERP PCA Toolkit [12]. Note that, unlike different ERP signals such as N200 and P300 the ERP subcomponents are temporally correlated. So, the spatial-PCA method, which has better performance for separation of temporally correlated, but spatially uncorrelated signals, is chosen as the benchmark for comparison [3].

Simulated data: The synthetic EEG data contains ERP signals in the interval between 250 and 500 ms after stimulus, respectively. Two highly overlapped P300 subcomponents, P3a and P3b are synthetically generated using gamma function [2]. A three-shell homogeneous head model was used to generate the EEG data. The sampling frequency was set to 250 Hz. The amplitudes, latencies, and widths of the P300 subcomponents varied across trials. The P3a was placed in centro-frontal and P3b in centro-parietal brain locations which makes them spatially close to each other. The goal of the simulation study was to evaluate the ability of the method in estimation of P300 subcomponents and their scalp projections in single trials with different SNR levels. The method was applied to different mixtures of synthetic sources (considering 30 trials) at different signal to noise ratios. The results for different experiments were found approximately similar when SNRs are the same. Generally, the optimization process converged after approximately 80 iterations. The average localization and source separation errors of the BSOS and PCA based methods are compared for 30 trials in three different SNR levels. The error of estimation is calculated by $err = 10log(\frac{||\mathbf{Z}-\hat{\mathbf{Z}}||^2}{||\mathbf{Z}||^2})$ where $\hat{\mathbf{Z}}$ represents correctly reordered and optimally scaled version of the any estimated $\mathbf{Z}$. Table I

TABLE I
Spatial error between original and separated P300 subcomponents in different SNRs.

SNR (dB)	0	-5	-10
BSOS error (dB)	**-23.24**±4.0905	**-14.77**±4.12	**-7.37** ±1.85
PCA error (dB)	-15.66±2.37	-5.67 ±3.05	-1.64±2.84

compares the averaged localization error for the two methods. Also, the averaged temporal error are shown in Table II. Clearly, in low SNR the proposed method outperforms the standard PCA based

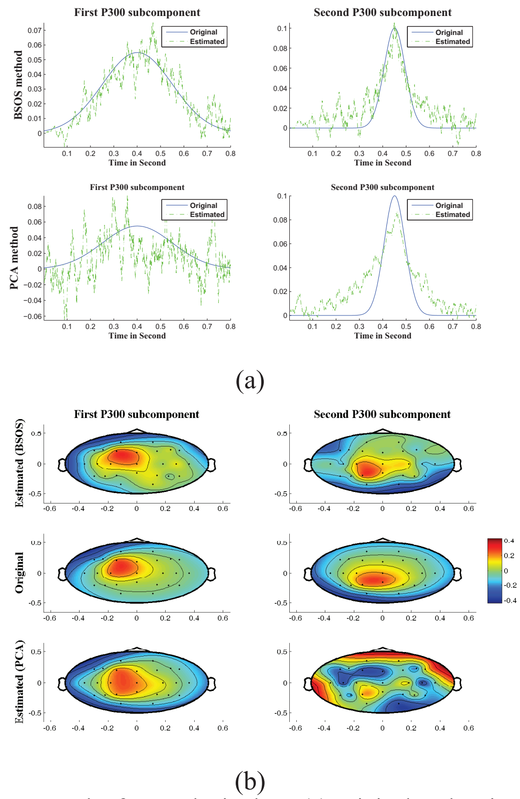

Fig. 1. Results for synthetic data; (a) original and estimated P300 subcomponents at SNR=-10dB, top left and right using proposed method (error=-23.28dB), bottom left and right using PCA based method (error=-7.80dB) and (b) original spatial information in the middle row, estimated spatial information using the proposed method (error=-8.86dB) and estimated spatial information using PCA based method (error=1.03dB) in the bottom row.

method for both channel estimation and signal separation. In high SNR, the signal separation error of the proposed method is slightly higher than the PCA based method, but in this case the channel estimation error is still better than that achieved by the PCA based method. So, as an alternative solution in high SNR cases the sources can be recovered using pseudo inverse of blindly estimated channel $\mathbf{A}$ and the electrode signals $\mathbf{X}$.

TABLE II
Temporal error between original and separated P300 subcomponents in different SNRs.

SNR (dB)	0	-5	-10
BSOS error (dB)	-28.98 ±2.21	**-26.05**±2.71	**-20.47**±2.78
PCA error (dB)	-33.45±2.46	-22.30±2.58	-9.88±5.77

Figure 1 compares the results of the proposed method and PCA based method in SNR=-10dB for estimating the subcomponents and their spatial information. Expectedly, the proposed method has shown better performance both spatial and temporal information in SNR=-10dB. Table III compares the latencies of estimated sources for both methods (The original latencies were chosen as 450 and 470 ms for first and second subcomponents respectively). Similar to the reported signal errors, the proposed method outperforms the PCA based method especially in low SNR.

TABLE III
Latencies of estimatted P300 subcomponents for different SNRs.

SNR (dB)	0	-5	-10
P3a by BSOS (ms)	450.38±0.71	448.16±4.73	455.93 ±6.64
P3a by PCA (ms)	449.79±0.66	454.09 ±7.29	461±12.84
P3b by BSOS (ms)	469.23±0.62	472.27±3.82	466.93 ±5.40
P3b by PCA (ms)	470.66±0.36	465.49 ±5.29	478±8.84

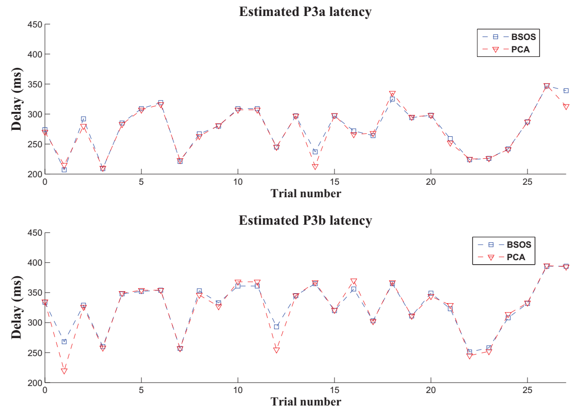

Fig. 2. Latencies of estimated P300 subcomponents signals, top P3a latencies using proposed method and PCA based method, bottom P3b latencies using proposed method and PCA based method

Real data: Real EEG was recorded using a Nihon Kohden model EEG-recorder system using 1kHz sampling frequency. EEG activity was recorded using 10-20 system by 27 electrodes. The signals were bandpass filtered between 0.1–40 Hz. Subjects were required to sit alert and still with their eyes closed to avoid any interference. The stimuli were transfered through ear plugs inserted in the ear. Thirty target tones (1 kHz) were randomly distributed amongst 160 frequent tones (2 kHz). Their intensity was 65 dB with 10 and 50 milliseconds duration for rare and frequent tones, respectively. The subject was asked to press a button when they hear a low tone (1 kHz). Each trial lasted 1300 ms and there was 500 ms prestimulus and 800 ms poststimulus. ERP subcomponents measured in this task included P3a and P3b using a temporal window which masks the trial data between [200ms–450ms] after the stimuli. The algorithm was applied to 30 target trials. The results for different trials were nearly consistent (except for 3 trials which might be related to the subject distraction). Interestingly the error of fitting process was often less than 10 percent (because of having low pass filter in preprocessing phase the noises are highly degraded). This means that this experiment can be considered as a high SNR case for which both methods have relatively the same results and efficiency for simulated data. Figure 2 shows the measured latencies of separated P3a and P3b signals using both methods. Both methods have close results for both P3a and P3b latency measurement. Figure 3 shows blindly estimated P3a and P3b signals and their spatial information in one of the single trials.

According to the simulated data results it is expected to obtain better performance of BSOS in low SNR compared with PCA-based approach.

V. Conclusions

In this paper, a new method for single trial blind estimation of ERP subcomponents is proposed. The method defines a new extended PARAFAC2 based tensor model which supports the correlation of the sources in its structure. The proposed method is robust against temporal and spatial correlation between the ERP subcomponents. Based on the defined tensor model, the fitting processes to estimate the Tucker1 core tensor model and the orthogonal part of segmented sources, $\mathbf{P}_k$, have been developed. In the presence of parametric and structural constraints, essentially unique solution for separation of ERP subcomponents is achieved. Using blindly estimated parameters of the proposed model, source separation and localization of the P300 subcomponents is performed. Based on the simulation results, the method is also robust against low SNR. Using the simulated signals specially for low SNR scenarios, it is shown that our method outperforms spatial PCA method. Consequently a better approximation of P300 subcomponents and their scalp projections has been obtained. The estimated scalp projections can be used for more detailed localization (3D localization) of P300 subcomponents in the brain too. The method was also applied to real data. The results were consistent with those of standard spatial PCA. The proposed method is useful for some applications which deal with variability of ERP subcomponents such as monitoring of mental fatigue, Alzheimer's, and drug infusion effects.

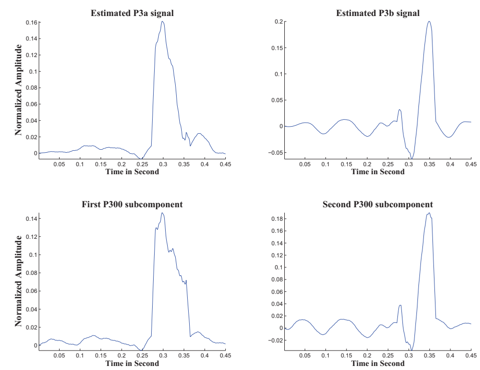

(a)

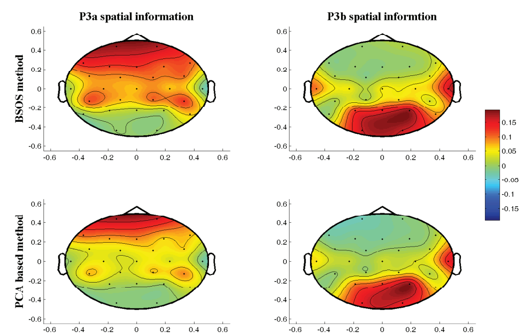

(b)

Fig. 3. Results for real data (a) Estimated P3a and P3b signals, top left and right using proposed method, bottom left and right using PCA based method and (b) estimated topographies of P3a and P3b signals, top left and right, using the proposed method, and estimated spatial information of P3a and P3b using PCA based method in the bottom row.

References

[1] J. Polich, "Clinical application of the P300 event-related brain potential.," *Physical medicine and rehabilitation clinics of North America*, vol. 15, no. 1, pp. 133–161, Feb. 2004.

[2] D. Jarchi, S. Sanei, J. C. Principe, and B. Makkiabadi, "A new spatiotemporal filtering method for single-trial estimation of correlated erp subcomponents," *IEEE Trans. on, Biomedical Engineering*, vol. 58, no. 1, pp. 132 –143, Jan. 2011.

[3] J. Dien, W. Khoe, and G. R. R. Mangun, "Evaluation of PCA and ICA of simulated ERPs: Promax vs. Infomax rotations.," *Hum. Brain. Mapp.*, Nov. 2006.

[4] E. Acar and B. Yener, "Unsupervised multiway data analysis a literature survey," *IEEE Trans. on knowledge and data engineering*, vol. 21, pp. 620, 2009.

[5] B. Makkiabadi, D. Jarchi, and S. Sanei, "Simultaneous localization and separation of biomedical signals by tensor factorization," *Proc. of IEEE Workshop on Statistical Signal Processing*, Sep. 2009.

[6] H. A. L. Kiers, J. M. F. Ten Berge, and R. Bro, "PARAFAC2 - Part I. A direct fitting algorithm for the PARAFAC2 model," *Journal of Chemometrics*, vol. 13, pp. 275–294, 1999.

[7] M. Weis, D. Jannek, F. Roemer, T. Guenther, M. Haardt, and P. Husar, "Multi-Dimensional PARAFAC2 component analysis of Multi-Channel EEG data including temporal tracking," Sept. 2010.

[8] R. Bro, "Multi-way analysis in the food industry," *PHD Thesis, Royal Veterinary and Agricultural University Denmark*, 1997.

[9] L. R. Tucker, *Implications of factor analysis of three-way matrices for measurement of change*, University of Wisconsin Press, Madison WI, 1963.

[10] R. Bro and S. De Jong, "A fast non-negativity-constrained least squares algorithm," *Journal of Chemometrics*, vol. 11, no. 5, pp. 393–401, 1997.

[11] N. J. Higham, "Computing real square roots of a real matrix," *Linear Algebra and its Applications*, vol. 88-89, pp. 405 – 430, 1987.

[12] J. Dien, "The ERP PCA Toolkit: An open source program for advanced statistical analysis of event-related potential data," *Journal of Neuroscience Methods*, Dec. 2009.